*Stanford Exploration Project, Report 111, June 9, 2002, pages 107–122*

# Velocity estimation for seismic data exhibiting focusing-effect AVO

*Ioan Vlad and Biondo Biondi*[1]

**ABSTRACT**

Transmission anomalies sometimes create AVO effects by focusing the reflected seismic wavefields, which impedes AVO analysis. The AVO anomalies caused by focusing are distinguishable by surface consistent patterns. We analyze the previous efforts to define, describe and eliminate spurious AVO anomalies. We also propose using wave equation migration velocity analysis to build an accurate velocity model. The transmission-related AVO can then be eliminated by downward continuation through this velocity model.

## INTRODUCTION

The phenomenon of amplitude variation with offset (AVO) of seismic reflection data is commonly assumed to occur only due to the petrophysical properties of the reflecting interfaces [Sheriff and Geldart (1995); Yilmaz (2001)]. However, amplitude can vary with offset due to absorption, or to focusing through velocity anomalies which are too small to give full triplications. The latter phenomenon has been shown to occur in several 2D [Kjartansson (1979); Harlan (1994)] and 3D (Hatchell, 2000a) seismic datasets. We will call it "focusing effect AVO" (FEAVO). FEAVO differs in two respects from regular AVO: 1) in CMP gathers, the high amplitudes are accompanied by local departures from hyperbolic moveout in the reflected arrivals (See Figure 1a); and 2) in the midpoint-offset space, the high amplitudes are distributed in "V" patterns whereas regular AVO gives rectangular patterns (See Fig. 1b). We must remove the FEAVO in order to allow AVO studies on FEAVO-affected data. Thus, it is necessary to:

Devise and prove the feasibility of a method whose application to FEAVO-affected 2D and 3D datasets would produce a velocity field accurate enough to generate a FEAVO-free prestack volume by downward continuing the wavefield through the FEAVO-generating anomalies.

## MOTIVATION

Most of the large structural onshore and shelf hydrocarbon plays have already been delineated, and seismic imaging efforts have begun to concentrate on subtler phenomena, such as those related to the presence of hydrocarbons in rocks. A resonant note is struck in crustal seismol-

[1]**email:** nick@sep.stanford.edu, biondo@sep.stanford.edu

ogy by the need to delineate the extent of lithospheric melts. AVO is one of the most common methods of characterizing the fluids in rocks in either exploration (Yilmaz, 2001) or crustal (Makovsky and Klemperer, 1999) surveys.

The FEAVO anomalies are much stronger than regular AVO effects, rendering AVO analysis impossible. Their removal will thus allow AVO analysis. A byproduct of the FEAVO removal process is a very accurate velocity model [White et al. (1988) shows that velocity contrasts as small as 2% can generate FEAVO], and this will also highly benefit AVO analysis, which is highly sensitive to the velocity used for prestack migration [Clapp (2002), Mora and Biondi (2000)].

FEAVO removal is also desirable for reasons beyond the obvious practical ones described above: in principle, the reflectivity that seismology seeks to recover is the high spatial frequency component of the impedance field. A FEAVO-contaminated image is simply inaccurate. Imaging the correct reflectivities is in line with the modern efforts towards true-amplitude imaging [Biondi (2001b); Sava and Biondi (2001a)]. And the by-product – an accurate velocity model describing the low spatial frequencies of the velocity field – is every bit as important as the reflectivity image itself (Claerbout, 1999).

## WHAT DO WE WANT TO DO?

We propose doing wave equation migration velocity analysis with a fitting goal specifically adapted to the nature of the FEAVO anomalies. This will provide a velocity model accurate enough so that we can eliminate the FEAVO effects by redatuming through it.

We will further describe the previous work on the recognition and removal of the FEAVO anomalies. We will lay down an approach to be undertaken in order to solve the problem defined in the second paragraph of this paper and we will evaluate the practical aspects of the implementation of the described approach. We will also describe the steps that we already undertook to solve the problem and the work that remains to be done, together with a time estimate for that.

## PREVIOUS WORK

### Work defining and describing the FEAVO effect

Kjartansson (1979) gives an example of the FEAVO effect on a real 2D dataset and interprets its physical meaning. Claerbout acknowledges the importance of the phenomenon by including a description and an explanation of it in his course notes (1982) and in his book, *Imaging the Earth's Interior* (1985). White et al. (1988) use forward modeling to show that FEAVO effects can be due to smooth velocity anomalies deviating by as little as 2% from the background velocity. The anomalies must be large compared to a wavelength but small when compared to the propagation distance. A solid case study (Hatchell, 1999) based on two real 3D datasets and on realistic forward modeling shows that not only shallow velocity anomalies can cause

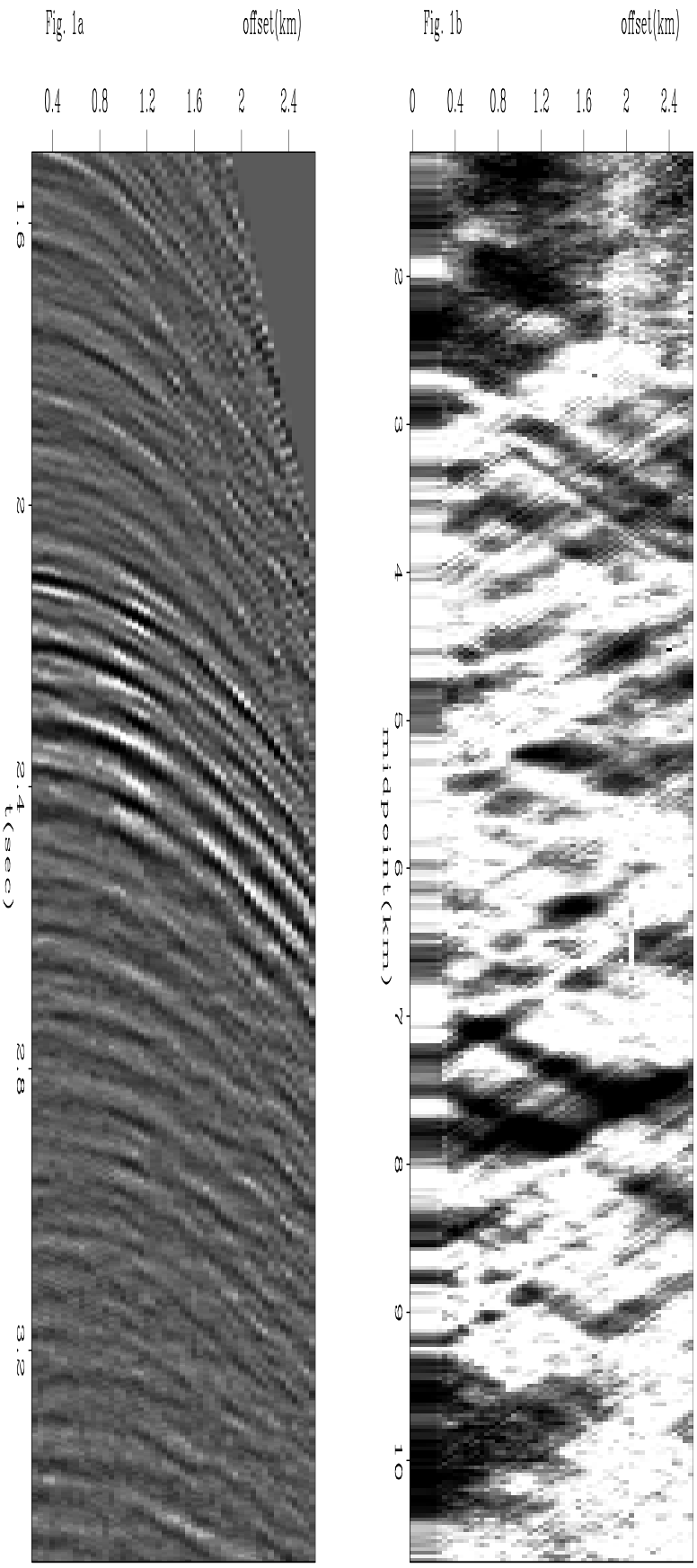


Figure 1: **a**: Part of a CMP gather exhibiting FEAVO anomalies. The strong event at 2.3s shows a slight departure from hyperbolic moveout, too subtle to allow successful classical traveltime tomography. **b**: FEAVO anomalies in the midpoint-offset space (Kjartansson "V"s). The preprocessing consisted in: muting, spherical divergence correction, bandpass filter, interpolation of missing or noisy traces, hydrophone balancing, f-k filtering, and offset continuation to fill in the small offsets (with a forward and inverse DMO cascade using the log-stretch DMO in the Fourier domain described in Zhou et al. (1996) and implemented by Vlad and Biondi (2001)). The figure has been produced exactely as in Kjartansson (1979): square and vertically stack the data between 1.5 and 3.5 seconds, then take the logarithm to increase the dynamic range. Offset continuation does not predict the FEAVO anomalies (the tips of the "V"s are not extended into the extrapolated small offsets) nick2-prodef [ER]

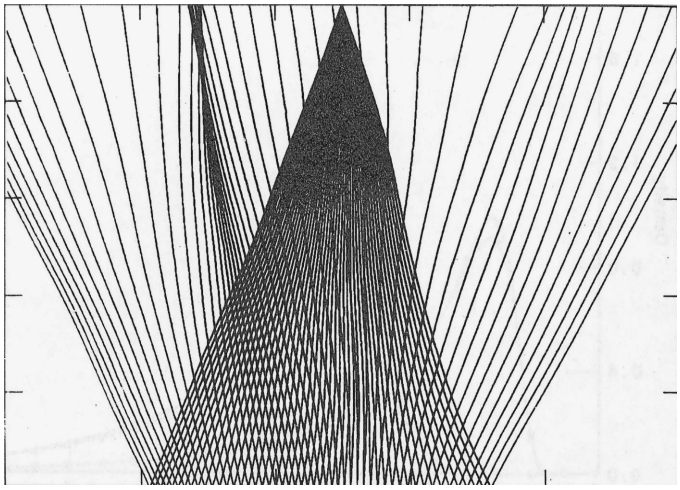

Figure 2: The physical explanation for the expression of FEAVO anomalies in CMP gathers (Figure 1a). If the frequency of the waves is high enough or the anomaly large enough, we will see a small triplication. Otherwise, only offset-dependant amplitude focusing (FEAVO) is visible. The traveltime delays are negligible, as the velocity anomaly changes only very little the length of the rays. Figure taken from White et al. (1988). nick2-whitebig [NR]

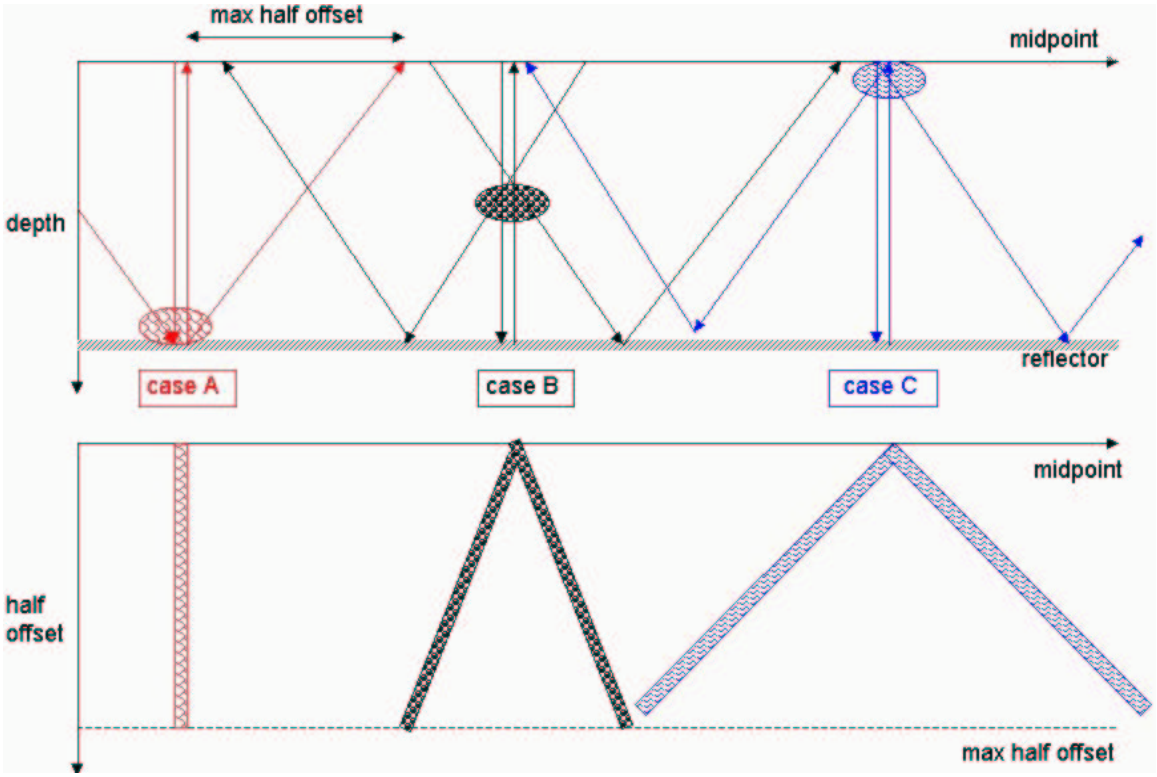


Figure 3: The physical explanation for the expression of FEAVO anomalies in midpoint-offset space (Kjartansson "V"s, Figure 1b). In the upper picture, the blobs are transmission anomalies and the arrows are raypaths for the zero offset and for the maximum offset recordings. For case A (anomaly on the reflector), only a single midpoint is affected, for all offsets. Case C (anomaly at the surface), is actually a static: its "footprint" is a pair of streaks slanting $45^o$ from the offset axis. Case B (in between) gives a pair of streaks with angles smaller than $45^o$. nick2-vilus [NR]

FEAVO effects; the sudden termination of a deep (3000m), low velocity layer by a fault can also be a source of focusing that affects the amplitudes more strongly than the traveltimes. This point draws interest: Hatchell (1999) received a Best Paper award at the SEG Annual Meeting and the idea is reiterated in Hatchell (2000a) and Hatchell (2000b).

### Attempts to invert FEAVO-affected data for a velocity model

Kjartansson (1979) not only recognizes the meaning of the FEAVO effect, but also takes a first step towards obtaining a velocity model. Taking into account that in the midpoint-offset space the opening angle of the "V"s depends on the depth of the transmission anomaly, he makes maps of the anomalies by slant stacking the power of the raw, unmigrated data. The maps adequately indicate the positions of the velocity anomalies but not the magnitudes. Claerbout (1993) refines this approach. In the frame of his work with prediction error filters at the time, he uses them to extend the Grand Isle dataset over a larger range of offsets. He also uses the new tool to compute a pilot trace that is crosscorrelated with the data. The traveltime anomalies are emphasized by plotting the times of the maximum values of the crosscorrelations in the midpoint-offset space.

Bevc (1993) generates a synthetic dataset exhibiting FEAVO anomalies and proposes a data-space tomography approach using downward continuation as the operator in tomography. This line of work is continued by Bevc (1994b), who shows using the synthetic that the FEAVO anomalies can indeed be eliminated by finding the velocity model, and then by downward continuing through it until under the FEAVO-causing velocity anomalies (redatuming). He also theoretically discusses inversion schemes. In the follow-up, Bevc (1994a) picks times from sags in the FEAVO-affected quasi-hyperbolic arrivals in CMP gathers and does traveltime tomography to find the velocity model. He operates under the assumption that the velocity anomalies are in the near surface. The tomography works in the following way: 1) apply NMO; 2) find the departures from the flatness of the events in CMP gathers (time lags) by crosscorrelating a pilot trace with the data; and 3) the lags are backprojected onto the velocity model that will be used for the NMO at the first step. The inversion in the last tomographic step uses a styling goal with PEFs. The method is shown to work on a simple synthetic dataset, but the conclusions contain a warning that it may not work on real data.

With a different approach (inverting picked maximum amplitudes and using ray-based operators), Harlan (1994) does not produce a velocity model, but a transmission anomaly section that is used to eliminate the FEAVO effect for a 2D dataset.

## PROPOSED APPROACH

We intend to eliminate the FEAVO anomalies by finding an accurate velocity model, then by downward continuing the data through it until under the FEAVO-causing velocity anomalies. The velocity will be found by migration velocity analysis (MVA), an iterative inversion process whose optimization goal is not fitting the recorded data, but providing the best focused migrated image (Biondi and Sava, 1999). The chapter pertaining to velocity analysis in Biondi

(2001a) shows (with examples) why dipping reflectors in laterally varying velocity media require the velocity analysis to be performed in the migrated domain (image domain) instead of the unmigrated domain (data domain). A wave-equation MVA (WEMVA) (Sava, 2000) will be used instead of a ray-based MVA (Clapp, 2001). The advantages of the former over the latter are detailed in the WEMVA chapter of Biondi (2001a). One particular advantage is the better treatment of amplitudes by wave-equation methods.

The usual WEMVA criterium describing the quality of the image is flatness in angle gathers. This is directly related to traveltime anomalies. As it is visible in Figure 1a, the traveltime changes associated with the FEAVO effect are very small and they do not produce curvatures in angle gathers. Biondi and Sava (1999) show on a synthetic, and this paper will show on a real dataset, that FEAVO anomalies keep their "V" shapes through prestack migration and conversion from offset to angle gathers. Therefore, the fitting goal of the inversion must be related to the distribution of amplitudes in the midpoint-angle space. The desired image will not exhibit these characteristic "V" patterns.

The inversion will proceed as follows: the wavefield at a certain depth is downward continued a depth step down through the known velocity model with an accurate (nonlinear) operator. The result is transformed to angle domain and a "perfect" image is created by eliminating the FEAVO anomalies. A image perturbation ($\Delta W$) is obtained by substracting the two images, and is backprojected through an invertible operator in order to obtain a velocity update ($\Delta s$). The velocity model is updated and the cycle proceeds again, until $\Delta W$ becomes negligible. The construction of the operator that links $\Delta s$ and $\Delta W$ is very important. The number of iterations and the accuracy of the result depends on its accurate invertibility. In order to make it invertible, Born (Sava and Biondi, 2001b) or other (Sava and Fomel, 2002) types of linearization are employed.

## COMPLETED STEPS TOWARDS THE STATED GOAL

Any iterative inversion process is built on three cornerstones: 1. The ability to transform a guess of the solution from the initial domain to a domain where an anomaly can be extracted; 2. The ability to extract the anomaly in this latter domain by comparing the result of the transformation of the initial guess against a set of criteria; and 3. The ability to transform the extracted anomaly back to the initial domain, updating the guess. In the particular case of the inversion we are setting up, the discrimination domain is the angle domain. We will further prove point 1 above: that the FEAVO anomalies are visible in the angle domain (that the common downward continuation followed by transformation from the offset to angle does not destroy them). We will also discuss point 2 (the various methods for extracting the FEAVO anomalies in the angle domain) but will leave an example of the actual extraction to a future paper. Because of time constraints, point 3 (proving that the linearized downward continuation does not spoil the anomalies) is also left for a future paper.

**Shallow-origin FEAVO effects are visible in the image domain**

Figure 1b shows a pattern of slanted symmetrical linear patterns (Kjartansson "V"s) that are the signature of FEAVO in the midpoint-offset domain. Figure 3 illustrates the way the patterns formed. The Kjartansson "V"s are a good way to discriminate the FEAVO anomalies in an inversion process. If we decide that the inversion discrimination will be done in the image domain, we need to make sure that the anomalies will not be destroyed by downward continuation. This was already shown on a synthetic in Fig. 5 of Biondi and Sava (1999). In order to show that the V-shaped patterns are visible as well in angle domain images produced from a real dataset, we migrated the Grand Isle prestack dataset then transformed to angle domain. The migration velocity depends only on depth (Figure 4), but not on midpoint (to avoid focusing by migration with an inappropriate velocity model). This assumption is close to the truth - Figure 5 shows that the geology is quite flat in the area. An examination of the midpoint-angle slices (Figure 6) reveals V-shaped patterns at the same locations as the data domain ones.

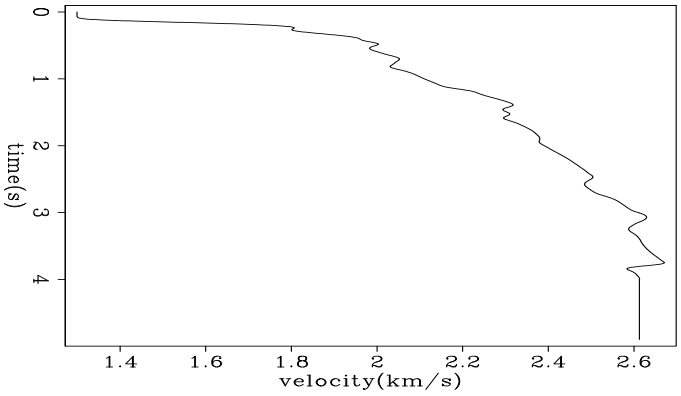


Figure 4: Interval velocity used in the migration of the Grand Isle dataset. The velocity does not depend on midpoint in order to not inadverdently focus the energy (the purpose of the migration is seeing whether the focusing anomalies are preserved). The *v(z)* assumption is close to geological reality in that area too. nick2-vint [ER]

**Deep-origin FEAVO effects can be modeled numerically**

Hatchell (2000a) proves using both real and synthetic data that FEAVO effects can be generated not only by shallow velocity anomalies, but also by deep ones. Figure 7 reproduces the forward modeling in Hatchell (2000a). A pseudospectral wave propagation algorithm (Biondi, 2002) is used to produce the wavefield recorded at a depth of 6000m. Ignoring the dispersion effects, the bottom two panels in the figure exhibit a striking quantitative similarity to the results in Hatchell (2000a) and emphasize that deep-origin FEAVO effects exist, and that they can be modeled numerically.

**Methods of extracting FEAVO effects in the angle gathers**

In order to invert, one must extract the anomalies. Since they are expressed both in the midpoint-angle domain and in the angle-domain common image gathers, their separation must proceed in a synergistic fashion. Figure 6 shows they bear a striking morphological resemblance to channels, so pattern-recognition techniques applied to a coherence volume (Marfurt

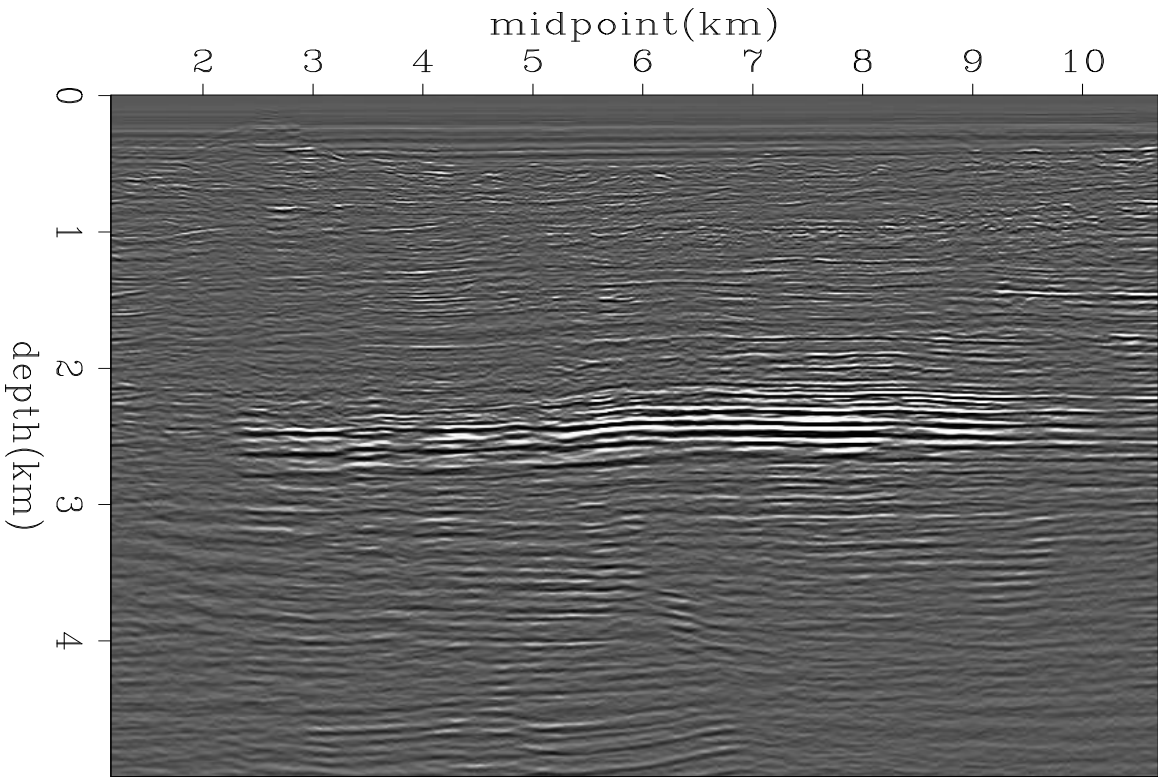


Figure 5: Migration (stack) of the Grand Isle dataset. The structure is quite flat. nick2-kimag [CR]

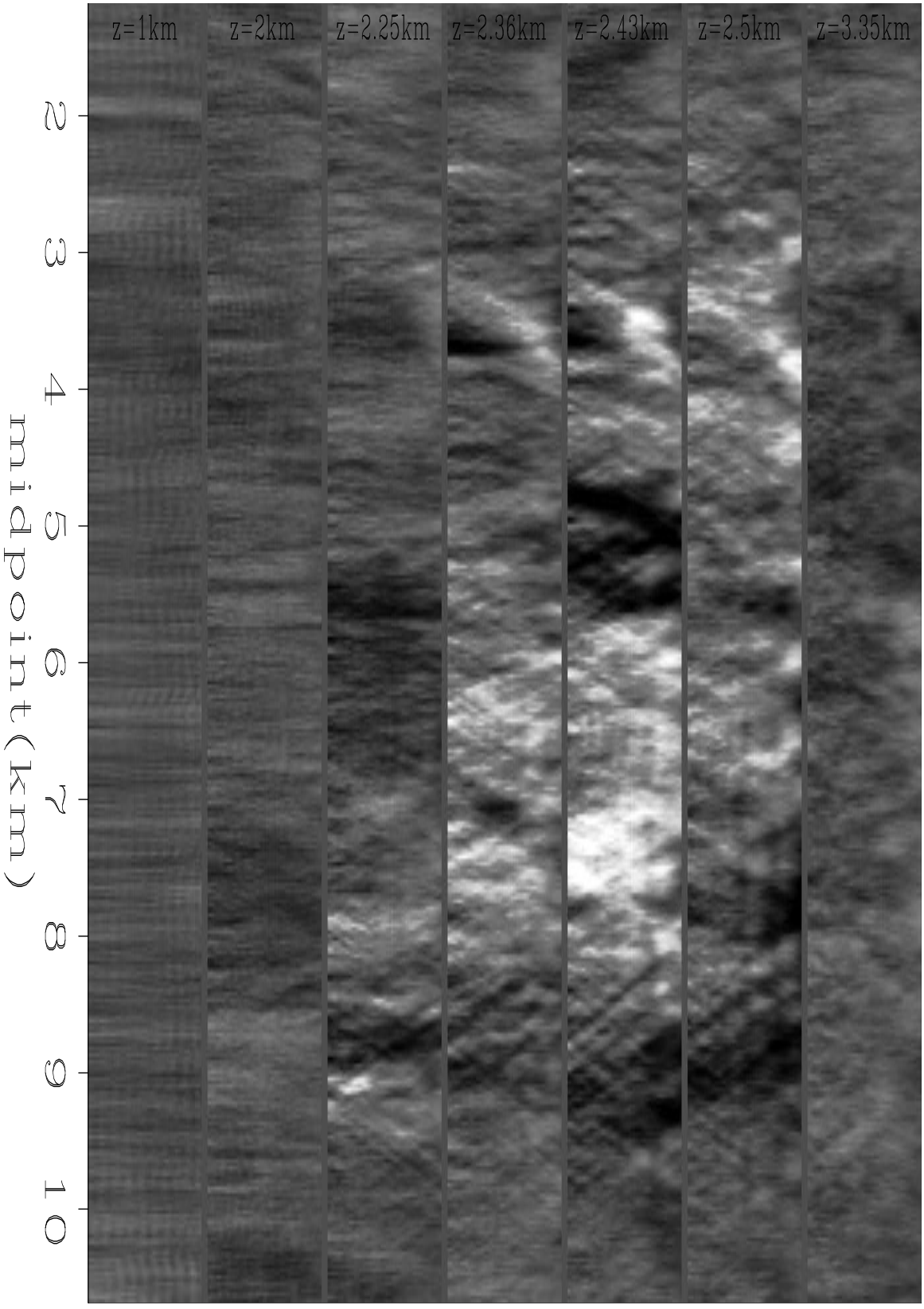


Figure 6: FEAVO anomalies in midpoint-angle depth slices. Each vertical panel shows the angle range between 0 and 20 degrees. The first panel (z=1km), the last (z=3.35km) and to a certain extent the second (z=2km) do not contain Kjartansson "V"s nick2-angpanel [CR]

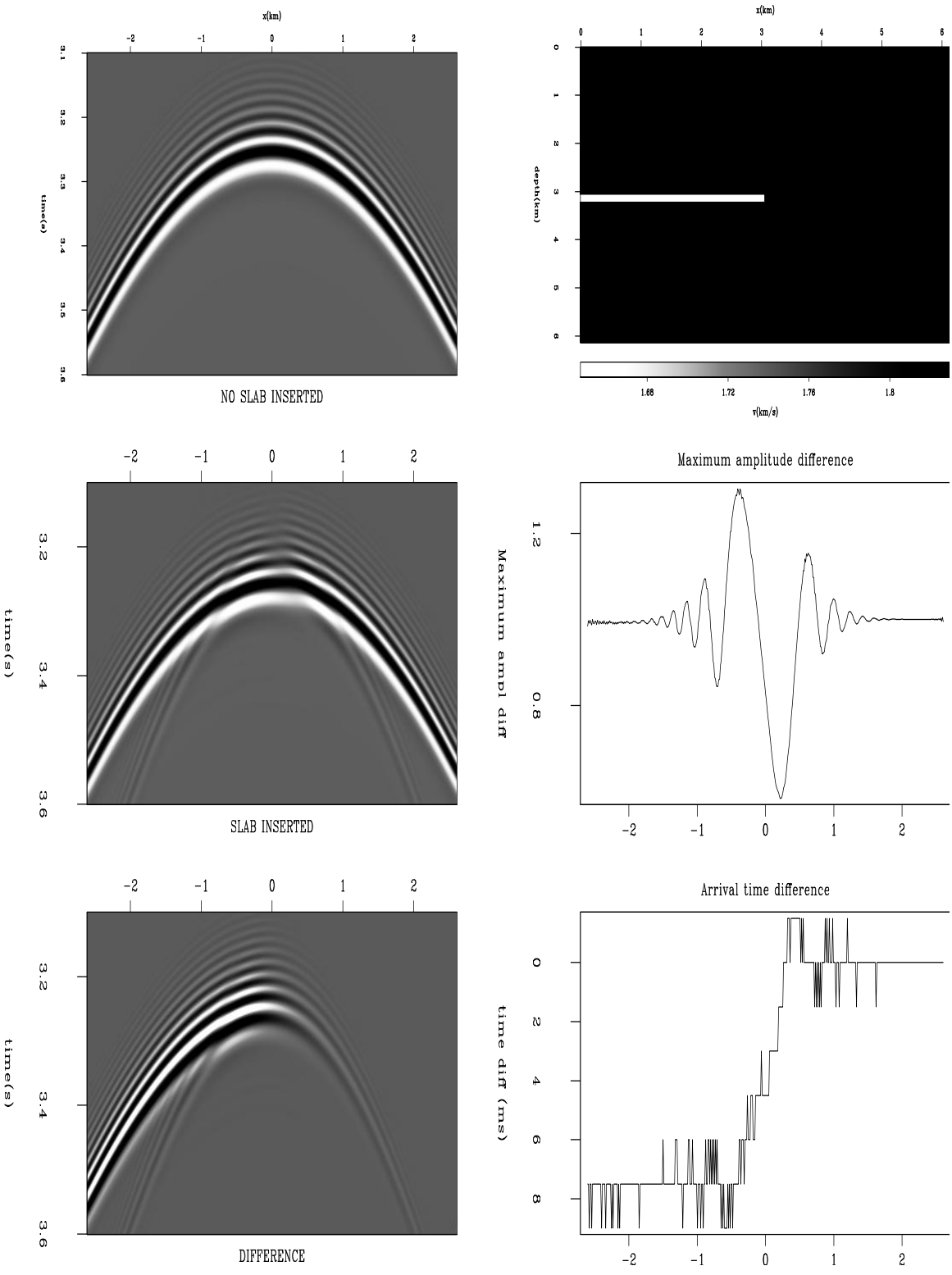


Figure 7: Left, from top to bottom: 1. Downward continuation of a shot from surface to 6 km deep, with constant velocity. 2. Downward continuation through upper right velocity model. 3. Difference between 1 and 2. Right, from top to bottom: 4. New velocity model — homogenous with a lower velocity slab inserted. 5. Difference between the maximum amplitudes in panel 1 and panel 2, for each x location. 6. Difference between the times of the maximum amplitudes in panels 1 and 2, for each x location. nick2-hatsim [CR]

et al., 1998) of the prestack cube may yield good results. Another way to discriminate them may be building a dip volume (Fomel, 2000) using plane-wave destructors (Claerbout, 1991). This may be successful because it is actually biomimicry: the human eye discriminates the anomalies based on their dip, or in the case of the data-domain hyperbola sags, on the discontinuities in the dip (dip derivative). These morphological approaches may be corroborated with spectral discrimination. In some cases, such as for the Grand Isle dataset, the FEAVO-causing velocity anomalies are small enough that different wavelengths may be affected differently (Figure 8).

## WORK TO BE DONE

In order to prove beyond reasonable doubt that an inversion is feasible, an actual extraction of the FEAVO anomalies in angle gathers should be performed. This should not pose any problems, amounting in the end to image processing - discriminating the anomalies based on their morphology. Since the third prerequisite for an inversion is an invertible operator, we should also show, at least on a particular case, that the linearized downward continuation operator preserves the FEAVO anomalies. Thus, after proving that an inversion for the velocity model that produces the FEAVO anomalies is possible, the work of setting up such an inversion first for 2D, then for 3D, remains to be done. The operators must be constructed and a reliable discrimination method in angle gathers set up.

We will approach the solution of the problem gradually, incorporating elements of complexity one by one. We first have to develop a process that will successfully separate the FEAVO anomalies in the angle domain, making them ready for input into an inversion scheme for obtaining $\Delta s$. We will then implement a 2D synthetic case, then a 2D real. We will develop the theory for the 3D case, build a 3D synthetic, implement a 3D synthetic case, then a 3D real one, and finally lay out the results in a publishable form.

## RESOURCES

### Seismic data

According to the strategy described in the previous section, we will use the following seismic datasets:

2D synthetic data: synthetic datasets exhibiting FEAVO effects have been generated in the past at SEP [Bevc (1993), Biondi and Sava (1999)] and due to research reproducibility, they can be easily obtained.

2D real data: the seismic line described in Kjartansson (1979). The dataset was acquired over the Grand Isle gas field offshore Louisiana and was made available to SEP in 1979 by Dr. Ralph Shuey (Gulf Science and Technology Company, at the time).

3D synthetic: After we prove the workability of the method in 2D, both on synthetic and

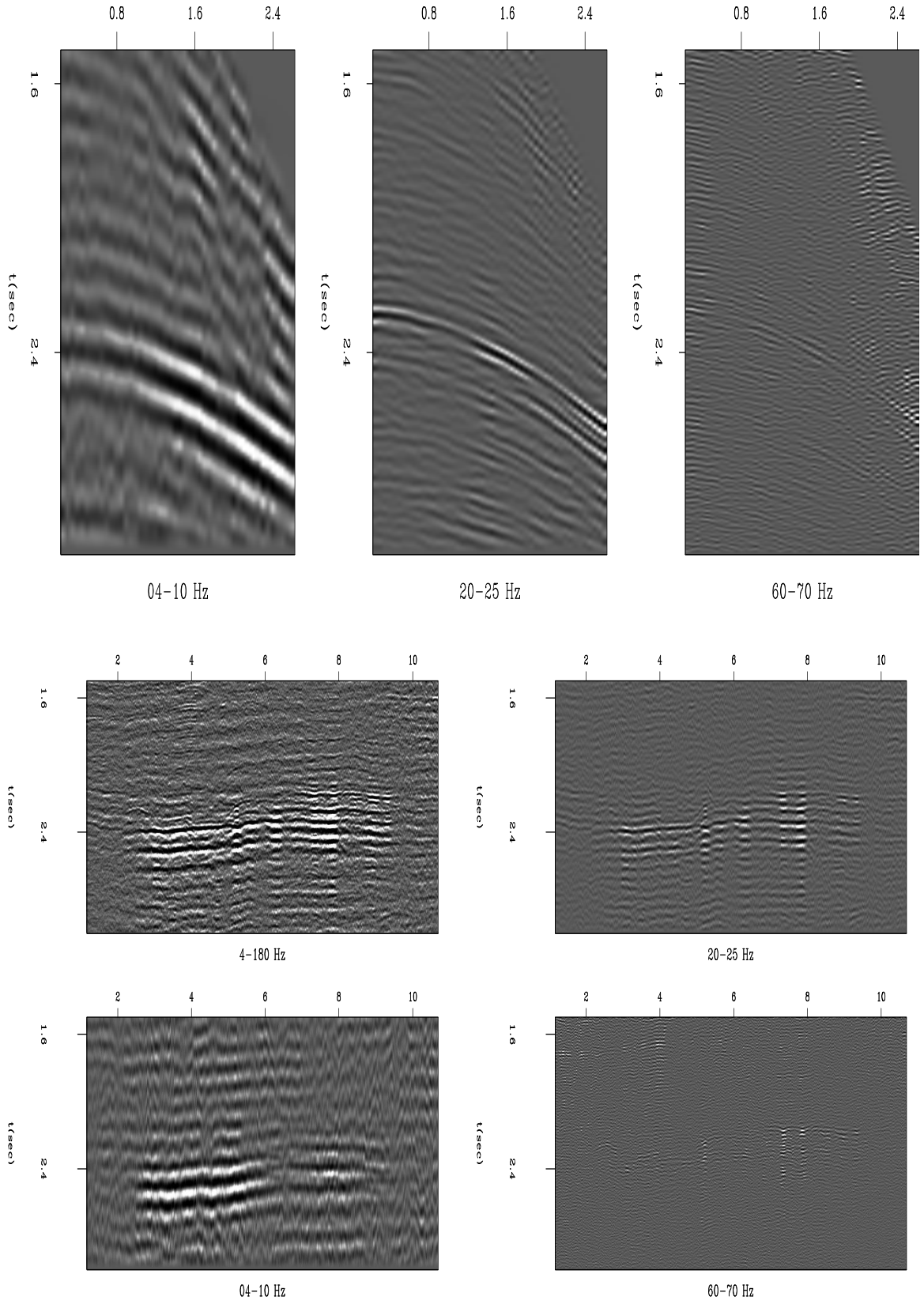


Figure 8: Top: CMP gather at 4.7 km, filtered with 4-10 Hz, 20-25 Hz, 60-70 Hz. Bottom: section with offset = 1.291km, filtered with 4-180 Hz, 4-10 Hz, 20-25 Hz, 60-70 Hz. Different frequency bands result in different extents of the FEAVO anomalies. nick2-kfdp [ER]

real data, we will generate a 3D synthetic data set exhibiting FEAVO anomalies.

3D real: Hatchell (2000a) has shown two examples of FEAVO-affected 3D datasets in the Gulf of Mexico, and by personal communication, we found out that there are other cases as well. We believe that once the proposed process shows its workability on a 3D synthetic, 3D real data can also be obtained.

### Software

Most of the software needed is already available at SEP. Besides elementary tools such as `Fortran90` compilers, `SEPlib`, `Matlab` and `Mathematica`, the $\Delta$Image-$\Delta$Slowness operator is already included in the `gendown` (Biondo Biondi) and `WEI` (Paul Sava) packages, already in existence at SEP. An out-of-core optimization library (`oclib`) for inverting large 3D datasets has already been written (Sava, 2001).

### Hardware

The proposed inversion scheme involves applying wave-equation migration to the data several times, so is therefore very computationally-intensive. Due to cluster technology, SEP has increased its computational power, but repeated prestack migrations of real 3D datasets, necessary for the final stages of this project, still need even more cluster nodes.

## ACKNOWLEDGEMENTS

Our thanks to Paul Sava for his help migrating and transforming to angle domain the Grand Isle dataset; to Bob Clapp for his advice and computer support; and to Brad Artman for the velocity analysis of the Grand Isle dataset.

## REFERENCES

Bevc, D., 1993, Toward estimating near surface lateral velocity variations: SEP–**79**, 69–78.

Bevc, D., 1994a, Datuming velocity from traveltime tomography: SEP–**82**, 145–164.

Bevc, D., 1994b, Near-surface velocity estimation and layer replacement: SEP–**80**, 361–372.

Biondi, B., and Sava, P., 1999, Wave-equation migration velocity analysis: SEP–**100**, 11–34.

Biondi, B. 3-d Seismic Imaging:. http://sepwww.stanford.edu/sep/biondo/Lectures, 2001.

Biondi, B., 2001b, Amplitude preserving prestack imaging of irregularly sampled 3-D data: SEP–**110**, 1–18.

Biondi, B., 2002, Reverse time migration in midpoint-offset coordinates: SEP–**111**, 149–157.

Claerbout, J. F., 1982, Imaging the Earth's Interior, chapters one to four: SEP–**30**, 233.

Claerbout, J. F., 1985, Imaging the Earth's Interior: Blackwell Scientific Publications.

Claerbout, J. F., 1991, Earth Soundings Analysis: SEP–**71**, 1–304.

Claerbout, J. F., 1993, Reflection tomography: Kjartansson revisited: SEP–**79**, 59–68.

Claerbout, J., 1999, Everything depends on v(x,y,z): SEP–**100**, 1–10.

Clapp, R. G., 2001, Geologically constrained migration velocity analysis: Ph.D. thesis, Stanford University.

Clapp, R. G., 2002, Effect of velocity uncertainty on amplitude information: SEP–**111**, 255–269.

Fomel, S., 2000, Applications of plane-wave destructor filters: SEP–**105**, 1–26.

Harlan, W. S., 1994, Tomographic correction of transmission distortions in reflected seismic amplitudes: 64th Annual Internat. Mtg., Soc. Expl. Geophys., Expanded Abstracts, 968–971.

Hatchell, P., 1999, Fault whispers: Transmission distortions on prestack seismic reflection data: 69th Annual Internat. Mtg., Soc. Expl. Geophys., Expanded Abstracts, 864–867.

Hatchell, P., 2000a, Fault whispers: Transmission distortions on prestack seismic reflection data: Geophysics, **65**, no. 2, 377–389.

Hatchell, P., 2000b, What causes distortions on prestack reflection seismic data?: World Oil, **221**, no. 11, 69–77.

Kjartansson, E., 1979, Analysis of variations in amplitudes and traveltimes with offset and midpoint: SEP–**20**, 1–24.

Makovsky, Y., and Klemperer, S., 1999, Measuring the seismic properties of Tibetan bright spots: Evidence for free aqueous fluids in the Tibetan middle crust: Journal of Geophysical Research, **104**, no. B5, 10795–10825.

Marfurt, K. J., Kirlin, R. L., and Farmer, S. L., 1998, 3-d seismic attributes using a semblance-based coherency algorithm: Geophysics, **63**, no. 04, 1150–1165.

Mora, C., and Biondi, B., 2000, Estimation of AVO attributes sensitivity to velocity uncertainty using forward modeling: A progress report: SEP–**103**, 349–366.

Sava, P., and Biondi, B., 2001a, Amplitude-preserved wave-equation migration: SEP–**108**, 1–26.

Sava, P., and Biondi, B., 2001b, Born-compliant image perturbation for wave-equation migration velocity analysis: SEP–**110**, 91–102.

Sava, P., and Fomel, S., 2002, Wave-equation migration velocity analysis beyond the Born approximation: SEP–**111**, 81–99.

Sava, P., 2000, A tutorial on mixed-domain wave-equation migration and migration velocity analysis: SEP–**105**, 139–156.

Sava, P., 2001, oclib - An out-of-core optimization library: SEP–**108**, 199–224.

Sheriff, R. E., and Geldart, L. P., 1995, Exploration Seismology: Cambridge University Press.

Vlad, I., and Biondi, B., 2001, Effective AMO implementation in the log-stretch, frequency-wavenumber domain: SEP–**110**, 63–70.

White, B. S., Nair, B., and Bayliss, A., 1988, Random rays and seismic amplitude anomalies: Geophysics, **53**, no. 07, 903–907.

Yilmaz, O., 2001, Seismic data analysis: processing, inversion and interpretation of seismic data: Society of Exploration Geophysicists.

Zhou, B., Mason, I. M., and Greenhalgh, S. A., 1996, An accurate formulation of log-stretch dip moveout in the frequency-wavenumber domain: Geophysics, **61**, no. 3, 17–23.